

Interband optical transition and electronic band structure of ferromagnetic EuB₆

Jungho Kim¹, C. C. Homes², B. K. Cho³, Young-June Kim¹, and E. J. Choi^{4,*}

¹*Department of Physics, University of Toronto, Toronto, Ontario M5S 1A7, Canada*

²*Department of Physics, Brookhaven National Laboratory, Upton, NY 11973-5000*

³*Center for Frontier Materials and Department of Materials Science and Engineering, K-JIST, Gwangju 500-712, Korea and*

⁴*Department of Physics and BK21 core program, University of Seoul, Seoul 130-743, Republic of Korea*

We obtained optical conductivity spectrum of EuB₆ over wide spectral range 2 meV–5.5 eV from reflectivity and spectroscopic ellipsometry measurements. A series of interband transition peaks are seen at high energy above 0.5 eV. Upon ferromagnetic ordering at 15.5 K, the interband transition peak intensity decrease strongly at three energy positions 0.5, 1.4, and 3 eV. The spectral weight is transferred to the Drude conductivity at low energy. In addition, the peak at 4 eV is seen to split in the ferromagnetic state. We found that all these spectral changes are explained coherently in a semimetallic band picture of EuB₆.

PACS numbers: 78.20.Ls, 78.40.Kc, 71.20.Eh, 71.70.Gm

The metallic europium hexaboride, EuB₆, has been studied intensively during the last decade due to the unusual transport and magnetic behaviors [1]. Like other rare-earth hexaboride such as CaB₆ and SrB₆, this material has a simple undistorted cubic structure consisting of B₆ cage and Eu ions. It has low density carrier ($\sim 10^{19}\text{cm}^{-3}$) and the 4f-magnetic moment of divalent Eu⁺² ($S=7/2$).

It was widely considered that EuB₆ is a semimetal, with the valence band (VB) and conduction band (CB) overlapping at the Fermi level. The de Haas-van Alphen and Shubnikov-de Hass experiments [2, 3] found the electron- and hole-pockets resulting from the semimetal band structure. Infrared-optical study of Eu_{1-x}Ca_xB₆ compounds [4] showed that the VB-CB overlap is about 0.3 eV in EuB₆. Band structure calculations using local density approximation (LDA) [5] and LDA+U [6] method predict that the band overlap occurs at the X point of the Brillouin zone.

On the other hand, angle-resolved photoemission spectroscopy (ARPES) experiments showed that EuB₆ is an insulator with a sizable gap [7, 8]. The CB and VB are separated by ~ 1 eV at the X-point. Similar result was obtained for isovalent CaB₆. This contradicting ARPES result might be attributed to a surface effect. In CaB₆, Denlinger *et al.* claimed that bulk-sensitive soft x-ray emission (SXE) and absorption (XAS) measurements reproduce the 1 eV gap [7]. In this insulator view of EuB₆, the metallic carriers are believed to come from crystalline defects. Such a long-standing controversy on the electronic band structure of EuB₆ remains an open question and awaits for further experimental study.

Europium hexaboride, EuB₆, undergoes a ferromagnetic (FM) transition at $T_c=15.5$ K [9]. At $T < T_c$, the resistivity drops sharply. Also in the infrared reflectivity measurement, the plasma frequency $\omega_p^2(\sim n/m)$ was found to increase [10]. These FM-induced changes indicate that the charge carriers are coupled with the mag-

netic moment in some ways. The enhanced metallicity was attributed to an increase of the carrier density (n) [11, 12] or independently to a reduction of the effective mass (m^*) [13]. As another possibility, a scenario of magnetic polarons near the transition temperature was considered [14, 15]. At present, it is not clear which mechanism is playing the major role.

In this Letter, we performed the first comprehensive optical spectroscopic experiment over the wide frequency range 2 meV–5.5 eV of EuB₆ using combined reflectivity and ellipsometry measurements. We observe a series of interband transitions at high energy up to ~ 5.5 eV and their remarkable spectral changes at the FM transition: intensity change at 0.5–3.3 eV region and absorption peak splitting at 4 eV. In far-infrared region (~ 0.1 eV), the increase of $\omega_p^2(\sim n/m)$ is reproduced. We could understand the three different changes coherently within a semimetal band picture. Our results provides a strong spectroscopic evidence that EuB₆ is a semimetal.

The single-crystal EuB₆ samples were synthesized by a boro-thermal flux method as described in Ref. 9 and characterized by x-ray diffraction, dc-resistivity and magnetization measurements [9, 16]. The normal incidence reflectivity, $R(\omega)$, was measured at $5\text{ K} \leq T \leq 100\text{ K}$ in the 2 meV–1 eV range using a Fourier transform spectrometer with an *in situ* overcoating technique [17]. For 0.7–5.5 eV range, optical dielectric constants were measured using spectroscopic ellipsometry (Woollam VASE ellipsometer). Throughout the measurement, sample temperature was controlled within 0.1 K of stability.

Fig. 1(a) shows $R(\omega)$ curves of EuB₆ for $5\text{ K} \leq T \leq 100\text{ K}$. The high reflectivity at low frequency region represents the metallic Drude response. The plasma edge shifts to higher energy as T decreases below $T=20$ K, consistent with the earlier observation by Degiorgi *et al.* [10, 18]. Fig. 1(b) presents the complex dielectric constants $\varepsilon_2(\omega)$ and $\varepsilon_1(\omega)$ obtained from the spectroscopic ellipsometry measurement. $\varepsilon_2(\omega)$ exhibits

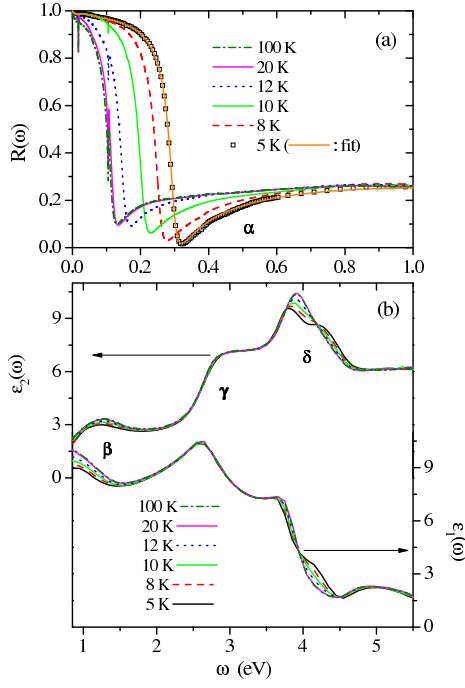


FIG. 1: (Color online) Optical spectra of EuB_6 for $T=5, 8, 10, 12, 20,$ and 100 K. (a) Reflectivity at $\omega < 1$ eV. (b) Dielectric constants, $\epsilon_2(\omega)$ and $\epsilon_1(\omega)$, for $0.7\text{--}5.5$ eV energy range from spectroscopic ellipsometry measurements. The peaks $\beta, \gamma,$ and δ represent the interband absorptions. α corresponds to the onset of the interband transitions. (see text)

three discernible peaks at 1.4 eV, 3 eV, and 4 eV. They represent interband electronic transitions and we label them as $\beta, \gamma,$ and δ , respectively. The peak heights of β and γ decrease slightly as T decreases. On the other hand, δ is shown to split into two peaks.

To better understand the T -dependent changes, we extract optical conductivity $\sigma_1(\omega)$ from $R(\omega)$ and $\epsilon_{1,2}(\omega)$ data. Here we used the fitting algorithm developed by Kuzmenko where $R(\omega)$ is fitted by a Kramers-Kronig (KK) constrained variational $\epsilon_1(\omega)$ and $\epsilon_2(\omega)$ [19]. Fig. 2(a) and (b) show $\sigma_1(\omega)$ of the Drude part and the high energy interband (IB) part, respectively. The Drude conductivity increases as T decreases. It reflects the blue-shift of the plasma edge. The IB $\sigma_1(\omega)$ consists of the absorption onset around 0.5 eV (α) and the two peaks (β, γ) in the region shown ($\omega < 3.3$ eV). As the insets show closely, $\sigma_1(\omega)$ at α, β and γ decreases as T decreases which is opposite to the Drude behavior. The changes at β and γ reflect directly those of $\epsilon_{1,2}(\omega)$ from ellipsometry measurement. The change of α arises from $R(\omega)$ above the plasma edge (at 0.1-0.6 eV) where the reflectivity level decreases as T decrease.

In Fig. 2(c), we show the difference $\Delta\sigma_1(\omega, T) = \sigma_1(\omega, T) - \sigma_1(\omega, 5\text{K})$ of the IB part. The decrease occurs at all frequency in addition to the three regions of strong changes. We calculate the spectral

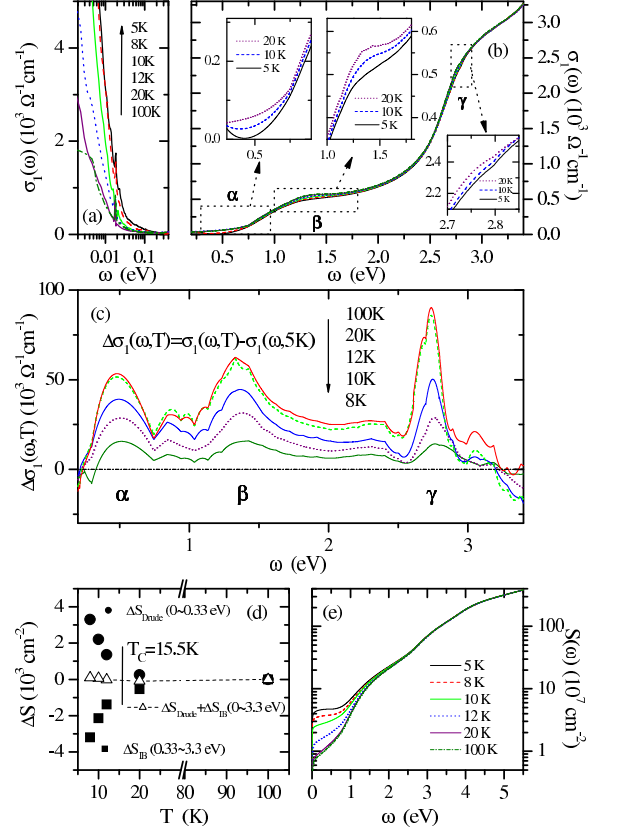


FIG. 2: (Color online) Optical conductivity $\sigma_1(\omega)$ of EuB_6 for (a) Drude part at $\omega < 0.4$ eV (b) interband (IB) part up to $\omega < 3.3$ eV. The insets of (b) show the expanded views of $\sigma_1(\omega)$. As T decreases, the Drude intensity increases while IB intensity decreases. (c) Difference of the IB conductivity $\Delta\sigma_1(\omega, T) = \sigma_1(\omega, T) - \sigma_1(\omega, 5\text{K})$. (d) Spectral weight change, $\Delta S = \frac{120}{\pi} \int_0^\omega [\sigma_1(\omega, T) - \sigma_1(\omega, 100\text{K})] d\omega$ for the Drude part, the IB part, and the sum of them. (e) Absolute spectral weight change, $S(\omega) = \frac{120}{\pi} \int_0^\omega \sigma_1(\omega) d\omega$ up to 5.5 eV.

weight change $\Delta S = \frac{120}{\pi} \int_{\omega_1}^{\omega_2} [\sigma_1(\omega, T) - \sigma_1(\omega, 100\text{K})] d\omega$ separately for Drude- and IB-parts where the area integration is taken for $0 < \omega < 0.33$ eV and $0.33 < \omega < 3.3$ eV, respectively. Fig. 2(d) shows that ΔS_{Drude} and ΔS_{IB} change significantly upon the FM transition. They approximately cancel each other, $\Delta S_{\text{Drude}} + \Delta S_{\text{IB}} \cong 0$. Fig. 2(e) shows the absolute spectral weight, $S(\omega) = \frac{120}{\pi} \int_0^\omega \sigma_1(\omega) d\omega$, up to 5.5 eV. The $\sigma_1(\omega)$ weight transfer is confined in the region below $\omega \sim 3.3$ eV and the optical sum rule is recovered at higher frequency. It shows that the spectral weight is transferred from the IB part to the Drude part. The observed change of IB part implies that the FM transition is accompanied by a significant change in the band structure.

The electronic structure of EuB_6 was studied theoretically by Massidda *et al.* [5] and Kuneš *et al.* [6]. In Fig. 3(a) and (b), we show the schematic band diagrams for paramagnetic (PM) and FM states, respec-

tively. The localized Eu 4f levels are at 1.3 eV below E_F [6] and are occupied by 7 electrons with parallel spin. The valence band (VB) and the conduction band (CB) are formed by hybridization of B 2p and Eu 5d orbitals. Among the five Eu 5d orbitals, $d_{x^2-y^2}$ hybridizes most effectively [6]. VB has mostly B 2p character while CB is dominated by Eu 5d character. VB and CB bands show semimetallic Fermi surface crossings at the X point of the Brillouin zone giving rise to free holes and electrons, respectively. The other Eu 5d orbitals are less hybridized and their bands are distributed at 3–7 eV above E_F . We show one of them at 3 eV. In this plot, we reproduce the result of Ref. 6 along the X- Γ and the X-M direction. We used the simple form $E_k = E_0 + W[\sin(k_x a/2) + \cos(k_y a/2)]$ to represent the bands while the real band dispersions are more complicated [20]. Turning to the optical transitions, the arrows A, B, and C represent possible interband excitations VB \rightarrow CB, Eu 4f \rightarrow CB, and VB \rightarrow Eu 5d. They all obey the dipole selection rule. We now simulate their absorption spectra $I(\omega)$ from $I(\omega) = 2 \cdot \int M_{fi}(k) \delta(\omega - \Delta E(k)_{fi}) dk$ where $M_{fi}(k)$ is the transition matrix from i -band to f -band at the k point of BZ, $\Delta E(k)$ is the energy difference $E(k)_f - E(k)_i$, and the prefactor 2 represents the up- and down-spin channels. In Fig. 3(c), we plot the calculated $I(\omega)$ for A, B and C in PM state (black curves). k was scanned along G-X-M line and $M_{fi}(k)$ was set to constant for simplicity.

In FM phase, the bands split into spin-up and spin-down sub-bands due to the exchange coupling to the local Eu 4f moments. For CB, Kuneš *et al.* showed that the spin-up band (parallel to the Eu 4f spin) moves down while the spin-down band (antiparallel) moves upward. As a result, their electron pocket expands (spin-up) or shrinks (spin-down). For VB, the interaction has opposite sign and the band shift occurs in the opposite direction. The Eu 5d band undergoes a similar splitting as the CB. The spin-splitting is large at X point, 0.3 eV for the CB and 0.2 eV for the VB.

The band splitting brings about interesting changes in the optical spectra of both the Drude and the IB part. The density of the spin-up electron in the CB will increase due to the enlarged Fermi surface while that of spin-down electrons decrease. The density change will take place for the VB holes also. This will result in a change of the plasma frequency which is given by $\omega_p^2 = 4\pi n/m_b$ for each band branch. Here density n is taken from the Fermi sphere volume ($n = k_F^3/3\pi^2$) and band mass m_b is estimated from the band dispersion. The total ω_p^2 is the sum of the four contributions, $\omega_p^2 = [\omega_p^2(\uparrow) + \omega_p^2(\downarrow)]_{CB} + [\omega_p^2(\uparrow) + \omega_p^2(\downarrow)]_{VB}$. We repeat it for PM state. The results shows $\omega_{p,FM}^2/\omega_{p,PM}^2 \sim 4.9$. The increase of ω_p^2 in FM comes mostly from the increase of n . For both hole and electron, the total (up+down) n becomes larger in FM. In experiment, we use the optical sum rule $\omega_p^2 = \frac{120}{\pi} \int_0^{\omega_c} \sigma_1(\omega) d\omega$ where $\omega_c = 0.33$ eV is

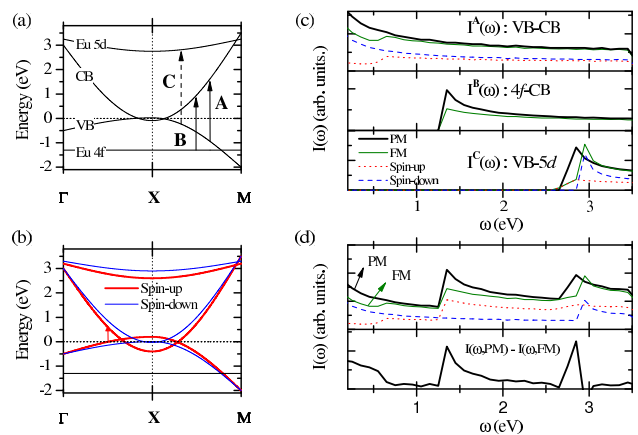


FIG. 3: (Color online) Schematic band structure of EuB_6 for (a) PM and (b) FM states. In (a), the arrows A, B, and C indicate optical transitions between the bands. In (b), the small arrow indicates A transition in spin-up channel. (c) Optical absorption spectrum $I(\omega)$ of the three interband transitions A, B, and C. $I(\omega)$ was calculated for PM and FM states using the band diagrams (a) and (b). The FM curves are resolved into spin-up and spin-down components. (d) Total optical transition $I(\omega) = I^A(\omega) + I^B(\omega) + I^C(\omega)$ (upper panel) and the difference of $I(\omega)$ between PM and FM states (lower panel).

taken. Taking $T=5$ K and 20 K data for FM and PM, we find $\omega_{p,FM}^2/\omega_{p,PM}^2 \sim 4.4$. The two results appear to be in reasonable agreement. It shows that the density increase is the primary source of the enhanced metallicity in the FM phase.

For IB transitions, we have to consider the spin-up and spin-down transition channels separately. For excitation A, let us consider the spin-up VB and spin-up CB. The former shifts upward and the electrons available for A transition (i.e. those with $E < E_F$) are reduced. As a result, the transition intensity will become weaker. The calculated $I(\omega)$ for spin-up A transition (top panel of (c), red dot curve), shows a suppression at low energy below 0.5 eV, since along the X- Γ the transition at $k=k_F$ has finite energy of 0.5 eV as indicated by the small arrow in Fig. 3(b). Below this onset energy, A is not allowed. Along the X-M, the change is less dramatic. For spin-down channel, the opposite behavior, i.e. the $I(\omega)$ increase will occur but the change is much weaker. The total $I(\omega)$ for A transition (solid green curve) shows that the intensity is reduced in FM phase due to the effect of the spin-up channel. We continue $I(\omega)$ calculation for the B and C transitions and find similar intensity reductions. The $I(\omega)$ decrease in B is due to the CB shift. Note that this transition occurs only through the spin-up channel. The change in C is due to the spin-up VB similar to A.

In Fig. 3(d), we show the total $I(\omega)$ spectrum (A+B+C) for the PM and the FM phases and the difference $I(\omega, \text{PM}) - I(\omega, \text{FM})$. The latter exhibits structures very similar to those observed in the experiment, Fig 2(c).

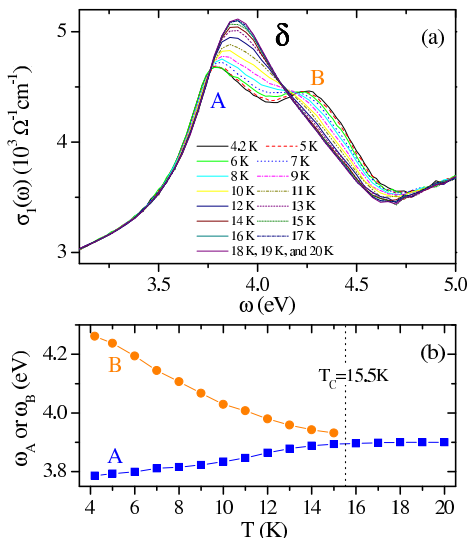


FIG. 4: (Color online) (a) Interband transition δ and its T-dependent changes for $T < 20$ K. (b) Peak positions below the splitting at $T_C = 15.5$ K.

This result strongly suggest that the three humps originate from the IB transitions (A, B, and C). The hump positions are in good agreement with data. Note that our calculation of $I(\omega)$ is very primitive, since we used a simplified band structure, and the k-dependence of $M_{ij}(k)$ was ignored. We also included only part of the k-space in our calculation. Nevertheless, our simple calculation reproduces essential features of the experimental observation very well: the Drude weight increase and the IB suppression. This result strongly supports the semimetallic band picture of EuB_6 .

In Fig. 4(a), we show the high energy feature δ at 4 eV. As T decreases, the peak splits into two sub-peaks. The peak position plot in (b) shows that the splitting is related to the onset of FM phase. At $T = 4.2$ K, the splitting amounts to 0.48 eV. We find that the spectral weight is conserved before and after the FM transition unlike α , β , and γ . We attribute δ to, among other possibilities, the transition from VB to a Eu 5d band. Eu 5d bands are distributed at $3 < E < 8$ eV and one of them is located at 3.5 eV above E_F (not shown in Fig. 3). It shows particularly strong spin-splitting by 0.5 eV at Γ point of the BZ [6]. The transition from VB to this Eu 5d band will occur at 4 eV and split at FM, consistent with the behavior of δ [21]. The band diagram predicts a similar spin-splitting of other Eu 5d bands at higher energy and we expect additional FM-induced peak splittings will exist above the range of our measurement.

When EuB_6 is regarded as insulator, the CB and VB are considered to be separated by 1 eV and the metallic carriers are induced by impurities. The 1 eV gap is inconsistent with the change of IB conductivity at around 0.5 eV. Also we showed that the the spectral weight transfer between the Drude and IB part comes naturally in the

semimetal band structure. In the insulator-view, however, this phenomenon is difficult to explain.

In summary, we obtained optical conductivity of the ferromagnetic hexaboride EuB_6 in the wide spectral range 0.002–5.5 eV through careful reflectivity and ellipsometry measurements. $\sigma_1(\omega)$ consists of the Drude conductivity at infrared region, three interband absorptions at $0.33 < \omega < 3.3$ eV and then a sharp peak at higher energy 4 eV. On the FM transition, the Drude weight increases and the interband absorption intensity decreases. The 4 eV peak splits into two peaks. We find that the spectral weight is transferred from the interband to the Drude part. The interband change is particularly strong at three energy positions 0.5, 1.4, and 3 eV. We employed a semimetallic band structure and analyzed the effect of exchange interaction driven spin-dependent band splitting in FM phase. The correlated changes of the Drude part and the interband part are successfully explained in detail. The behavior of the 4 eV peak is also accounted for in this picture. Our results provides a strong spectroscopic evidence that EuB_6 is a semimetal.

This work was supported by the KRF Grant No. - 070-C00032 and the KOSEF through CSCMR. The work at Toronto was supported by NSERC Discovery Grant & Research Tools and Instrumentation grant. Work at Brookhaven National Laboratory was supported by the DOE under Contract No. DE-AC02-98CH10886.

* Corresponding author: echoi@uos.ac.kr

- [1] C. N. Guy, S. von Molnar, J. Etourneau, and Z. Fisk, Solid State Commun. **33**, 1055 (1980).
- [2] R. G. Goodrich, N. Harrison, J. J. Vuillemin, A. Teklu, D. W. Hall, Z. Fisk, D. Young, and J. Sarrao, Phys. Rev. B **58**, 14896 (1998).
- [3] M. C. Aronson, J. L. Sarrao, Z. Fisk, M. Whittton, and B. L. Brandt, Phys. Rev. B **59**, 4720 (1999).
- [4] J.-H. Kim, Y. Lee, C. C. Homes, J.-S. Rhyee, B. K. Cho, S.-J. Oh, and E. J. Choi, Phys. Rev. B **71**, 075105 (2005).
- [5] S. Massidda, A. Continenza, T. M. D. Pascale, and R. Monnier, Z. Phys. B **102**, 83 (1997).
- [6] J. Kuneš and W. E. Pickett, Phys. Rev. B **69**, 165111 (2004).
- [7] J. D. Denlinger, J. A. Clack, J. W. Allen, G.-H. Gweon, D. M. Poirier, C. G. Olson, J. L. Sarrao, A. D. Bianchi, and Z. Fisk, Phys. Rev. Lett. **89** (2002).
- [8] S. Souma, H. Komatsu, T. Takahashi, R. Kaji, T. Sasaki, Y. Yokoo, and J. Akimitsu, Phys. Rev. Lett. **90** (2003).
- [9] J.-S. Rhyee, B. K. Cho, and H.-. C. Ri, Phys. Rev. B **67**, 125102 (2003).
- [10] L. Degiorgi, E. Felder, H. R. Ott, J. L. Sarrao, and Z. Fisk, Phys. Rev. Lett. **79**, 5134 (1997).
- [11] M. Kreissl and W. Nolting, Phys. Rev. B **72**, 245117 (2005).
- [12] C. Lin and A. J. Millis, Phys. Rev. B **71**, 075111 (2006).
- [13] J. E. Hirsch, Phys. Rev. B **62**, 14131 (2000).
- [14] P. Nyhus, S. Yoon, M. Kauffman, S. L. Cooper, Z. Fisk, and J. Sarrao, Phys. Rev. B **56**, 2717 (1997).

- [15] S. Süllow, I. Prasad, M. C. Aronson, S. Bogdanovich, J. L. Sarrao, and Z. Fisk, Phys. Rev. B **62**, 11626 (2000).
- [16] J.-S. Rhyee, B. H. Oh, B. K. Cho, H. C. Kim, and M. H. Jung, Phys. Rev. B **67**, 212407 (2003).
- [17] C. C. Homes, M. Reedyk, D. A. Crandles, and T. Timusk, Appl. Opt. **32**, 2976 (1993).
- [18] S. Broderick, B. Ruzicka, L. Degiorgi, H. R. Ott, J. L. Sarrao, and Z. Fisk, Phys. Rev. B **65**, 121102(R) (2002).
- [19] A. B. Kuzmenko, Rev. Sci. Instrum. **76** (2005).
- [20] In our plot of the PM state, (E_0, W) values for CB&VB along X- Γ and along X-M are $(6.1, -3.1)_{CB}$ & $(-1.02, 0.52)_{VB}$ and $(7.1, -3.6)_{CB}$ & $(-4.02, 2.02)_{VB}$, respectively. (E_0, W) for Eu 5d at 3 eV is (3.3, -0.5).
- [21] The transition from Eu 4f to Eu 5d (~ 3 eV) is another possible source for δ . We find from the peak fitting that δ at the PM state consists of at least 2 Lorentzian peaks suggesting multiple origins of δ .